

Measurement of charged jet cross sections and jet shapes in proton-proton collisions at $\sqrt{s} = 2.76$ TeV with the ALICE detector at LHC

Rathijit Biswas for the ALICE Collaboration

Centre for Astroparticle Physics and Space Science, Bose Institute, Kolkata, India
rathijit.biswas@cern.ch

Abstract. We present measurements of charged jet cross sections and jet shape observables in leading jet in proton-proton (pp) collisions at $\sqrt{s} = 2.76$ TeV with the ALICE detector at LHC. Jets are reconstructed at midrapidity from charged particles using the sequential recombination anti- k_T jet finding algorithm for various R values. The results are compared to measurements from HERWIG, PHOJET and different tunes of PYTHIA6 and earlier measurements at 7 TeV.

Keywords: Charged jet, jet shape, ALICE

1 Introduction

Jets are defined as the collimated stream of final state hadrons, produced from the fragmentation of hard scattered partons (quarks and gluons) in high energy collisions. Jets serve as tool to connect the final state hadrons with the primarily produced partons and thus they are probe to test perturbative quantum chromodynamics (pQCD). The study of jet shapes provides details of the parton to jet fragmentation with insight to jet tranverse profile. Furthermore, the measurements in pp serves as a baseline reference for similar measurements in heavy-ion (AA) collisions, where a highly dense medium is created, to isolate the hot matter effects.

2 Data analysis, jet reconstruction and observables

For this analysis, 4.4×10^7 minimum bias events recorded by the ALICE detector at the Large Hadron Collider (LHC) during 2011 are used. Events with primary vertex within ± 10 cm along the beam axis from the geometrical interaction point are analysed. Charged tracks are reconstructed using the combined information from Time Projection Chamber (TPC) and Inner Tracking System (ITS) and tracks with $p_T^{track} > 150$ MeV/c, $|\eta^{track}| < 0.9$ are selected for the analysis. Jets are reconstructed using sequential recombination anti- k_T [1] jet clustering algorithm from the FastJet package [2]. The differential charged jet cross sections

are measured with $R = 0.2, 0.3, 0.4$ and 0.6 using the equation

$$\frac{d^2\sigma^{jet,ch}}{dp_T d\eta}(p_T^{jet,ch}) = \frac{1}{\mathcal{L}^{int}} \frac{\Delta N_{jets}}{\Delta p_T \Delta \eta}(p_T^{jet,ch}) \quad (1)$$

where \mathcal{L}^{int} is the integrated luminosity (1.3 nb^{-1} in our case) and ΔN_{jets} the number of jets in the selected intervals of Δp_T and $\Delta \eta$. Jet shape observables such as average numbers of charged tracks in a leading jet ($\langle N_{ch} \rangle$), leading charged jet size (average radius containing 80% of the total jet p_T , $\langle R_{80} \rangle$) and radial distribution of p_T density about the jet axis (dp_T^{sum}/dr) are measured for $R = 0.4$.

3 Corrections and systematic uncertainties

The jet p_T spectra are corrected for instrumental effects by the Bayesian unfolding technique [3] using Monte Carlo (MC) events and full detector simulation with GEANT3 [4]. Jet shape observables are corrected using a bin-by-bin correction technique. All the observables are further corrected for the contribution of the underlying event (UE) from sources other than hard scattering. The UE is estimated following the technique used by ALICE [5] and subtracted event-by-event for jet p_T spectra and on a statistical basis for jet shape observables. The sources of systematic uncertainties include finite efficiency and momentum resolution, UE estimation and the dependence of correction factors on MC event generators.

4 Results

Figure 1 shows jet production cross sections for $R = 0.2, 0.3, 0.4$ and 0.6 (top), the $\langle N_{ch} \rangle$ distribution for $R = 0.4$ (bottom left) and the $\langle R_{80} \rangle$ distribution for $R = 0.4$ (bottom right) as a function of jet p_T . $\langle N_{ch} \rangle$ increases monotonically with increasing jet p_T as seen in earlier measurements. $\langle R_{80} \rangle$ is contained within half of the total radius for the lowest jet p_T , and it decreases for higher jet p_T . Different MC models such as HERWIG, PHOJET and different tunes of PYTHIA6 describe the data reasonably well. The results for $\langle N_{ch} \rangle$ and $\langle R_{80} \rangle$ at 2.76 TeV are also compared to earlier measurements at 7 TeV (Fig. 2, top left and right) and as such we do not see any \sqrt{s} dependence within uncertainties. Figure 2 (bottom left) shows radial momentum distributions for four different jet p_T bins as a function of distance from the jet axis. $\langle dp_T^{sum}/dr \rangle$ is largest near the jet axis and it decreases towards the periphery. The measurements from various MC models are in good agreement with the data as shown in Fig 2 (bottom right).

5 Conclusions

We reported measurements of charged jet cross section for $R = 0.2, 0.3, 0.4$ and 0.6 and jet shapes for $R = 0.4$ in pp collisions at 2.76 TeV with ALICE.

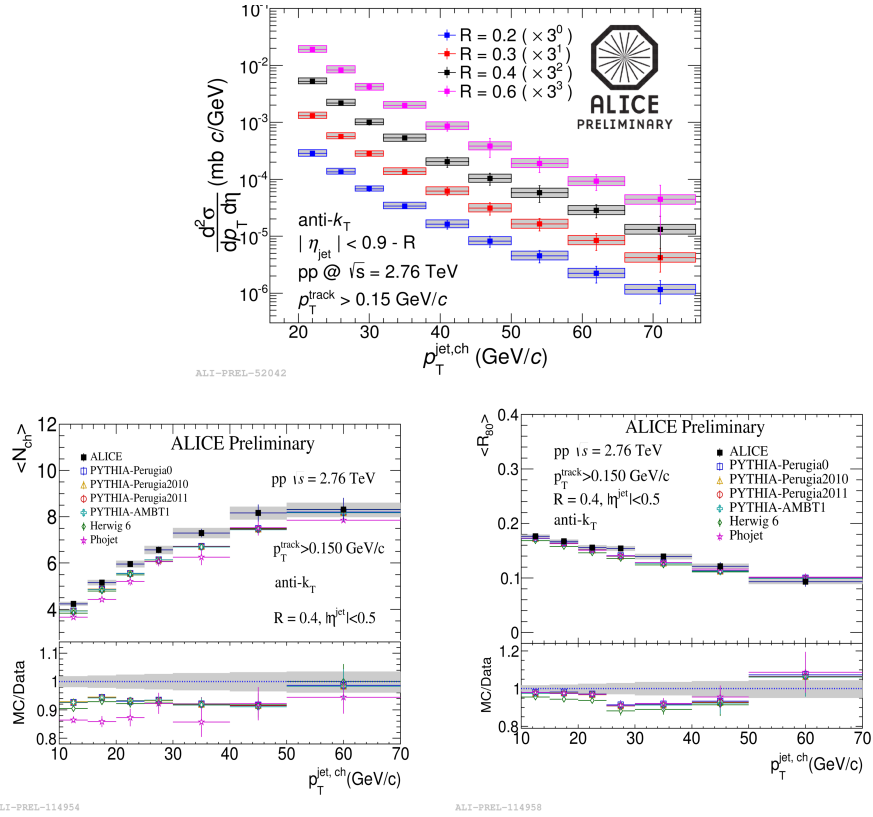


Fig. 1. Top: Charged jet production cross sections for $R = 0.2, 0.3, 0.4$ and 0.6 . Bottom left: $\langle N_{ch} \rangle$ distributions for $R = 0.4$ with different MC generator predictions and their ratios. Bottom right: $\langle R_{80} \rangle$ distributions for $R = 0.4$ with different MC generator predictions and their ratios. The vertical error bars in data and MC stand for statistical errors. The boxes and the grey bands show the systematic uncertainties.

$\langle N_{ch} \rangle$ increases with increasing jet p_T . Measurements of $\langle R_{80} \rangle$ and dp_T^{sum}/dr reveal that high p_T jets are more collimated. Various MC models well reproduce the data within uncertainties except $\langle N_{ch} \rangle$ which agrees within 15%. No \sqrt{s} dependence is seen within the measured uncertainties.

References

1. Cacciari M, Salam G P and Soyez G, JHEP 0804 (2008) 063
2. M. Cacciari and G. P. Salam, Phys.Lett.B 641 (2006) 5761
3. G. DAgostini, Nucl.Instrum.Meth.A 362 (1995) 487498
4. R. Brun, F. Carminati, and S. Giani, CERN-W5013, CERN-W-5013, <https://cds.cern.ch/record/1082634>
5. ALICE Collaboration, JHEP 1207 (2012) 116

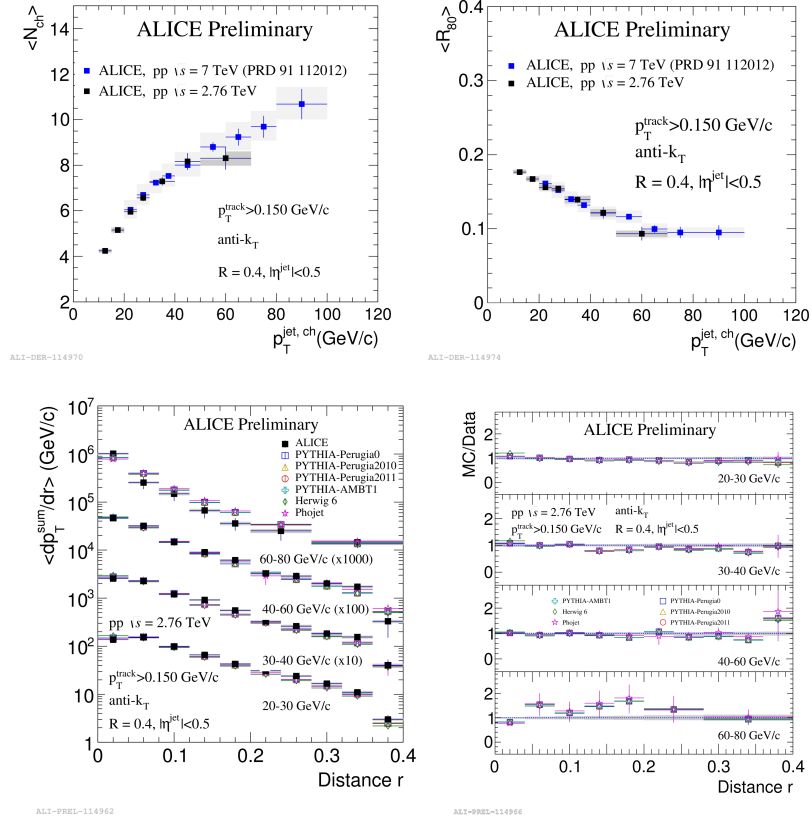


Fig. 2. $\langle N_{ch} \rangle$ (top left) and $\langle R_{80} \rangle$ (top right) at 2.76 TeV in comparison with that at 7 TeV. Bottom left: p_T^{sum} distributions for different jet p_T bins for $R = 0.4$ with different MC generator predictions. Bottom right: Ratios MC/data. The vertical error bars in data and MC stand for statistical errors. The grey bands show the systematic uncertainties.